ISSN 0965-5441, Petroleum Chemistry, 2019, Vol. 59, No. 5, pp. 540–545. © Pleiades Publishing, Ltd., 2019.
Russian Text © The Author(s), 2019, published in Nanogeterogennyi Kataliz, 2019, Vol. 4, No. 1, pp. 58–63.

Dealumination of Nanosized Zeolites Y

A. V. Yakimov[a, *], D. S. Zasukhin[a], V. A. Vorobkalo[a], O. A. Ponomareva[a, b], E. E. Knyazeva[b], V. I. Zaikovskii[c, d], B. A. Kolozhvari[a], and I. I. Ivanova[a, b]

[a] *Faculty of Chemistry, Moscow State University, Moscow, 119991 Russia*
[b] *Topchiev Institute of Petrochemical Synthesis, Russian Academy of Sciences, Moscow, 119991 Russia*
[c] *Boreskov Institute of Catalysis, Russian Academy of Sciences, Novosibirsk, 630090 Russia*
[d] *Novosibirsk State University, Novosibirsk, 630090 Russia*
**e-mail: alex.yakimov.20@yandex.ru*

Received October 2, 2018; revised October 26, 2018; accepted January 14, 2019

Abstract—The dealumination of nanosized zeolites is an important scientific problem, which should be solved to improve the activity of catalysts based on this zeolite in a broad range of heterogeneous catalytic reactions, particularly in commercial processes. However, the smaller the required size of the synthesized crystals, the lower the Si/Al ratio and the lower the degree of dealumination of this material can be achieved. In this study, the dealumination of zeolites Y with a crystal size of 50–1100 nm by treatment with ammonium hexafluorosilicate and steam heat treatment is discussed. It is shown that the dealumination with ammonium hexafluorosilicate is a "gentler" method in terms of structure preservation, whereas the dealumination by steam heat treatment provides a higher Si/Al ratio in the products; however, this method is inapplicable for crystals smaller than 500 nm, because it leads to the complete degradation of the structure. However, nanosized crystals can be dealuminated by treating with ammonium hexafluorosilicate. In this case, the degree of dealumination is close to 40%. A significant disadvantage of this method is the formation of a SiO_2 film on the crystal surface; this feature substantially restricts the use of the ammonium hexafluorosilicate treatment in the synthesis of cracking catalysts.

Keywords: nanosized zeolites, zeolite FAU(Y), dealumination, crystal size

DOI: 10.1134/S0965544119050116

Zeolites of the FAU(Y) structural type are widely used as an active component of catalysts for a broad range of commercial processes, such as cracking, hydrocracking, and isomerization of heavy alkanes [1, 2]. Typically, zeolites Y are synthesized by the hydrothermal crystallization of alkaline silica–alumina hydrogels with addition of seeds, which act as crystallization nuclei, to increase phase purity of product [3–6]. The SiO_2/Al_2O_3 ratio that can be achieved in the final product of this synthesis is 3–5 [5]. However, these materials cannot be used as catalyst components, because they are stable only in the Na form. The H form of zeolites Y with this composition undergoes amorphization [6].

To provide stability and decrease the number of strong Brønsted sites in the zeolite, it is subjected to dealumination, which leads to an increase in the SiO_2/Al_2O_3 molar ratio to 20–30. Thus, dealumination is an important stage in the preparation of catalysts based on zeolite Y, because it provides a simultaneous control of the stability and acidity of the zeolite. There are several zeolite dealumination methods that are based on two main approaches: (i) leaching of aluminum from the framework with the subsequent healing of defects and (ii) isomorphous substitution of Si for Al in the presence of chelating agents. The first approach is based on acid treatment [7–9], steam heat treatment (SHT) [9, 10], or their combination. In the second approach, the zeolite is treated with solutions of ammonium hexafluorosilicate (AHFS) and other silicon-containing agents [11, 12].

An important limitation imposed on the dealumination of zeolites Y is the crystal size. Zeolite Y with nanosized crystals is of the greatest interest for the synthesis of commercial catalysts, because the use of those materials allows to overcome diffusion limitations for large feedstock molecules [13]. Therefore, implementation of the dealumination of nanocrystalline zeolite materials is an important scientific and applied problem. However, in connection with the fact that the synthesis of nanocrystalline zeolites commonly occurs from reaction mixtures with high $[OH^-]/SiO_2$ molar ratios, the resulting nanocrystalline zeolites Y have a low SiO_2/Al_2O_3 ratio (3.0–3.5) because of partial silicon leaching during crystallization. In addition, the use of standard dealumination procedures based on SHT and acid treatment commonly leads to the rapid amorphization of nanocrystals.

According to [14], the dealumination of zeolites Y with a crystal size of less than 300 nm is hardly possible at all.

This study is focused on the effect of the crystal size of zeolites Y on the dealumination procedure the search for a dealumination method for zeolites Y with a crystal size of less than 300 nm. We used the following dealumination methods: a combined method based on the consecutive SHT and acid treatment procedures and isomorphous substitution in the presence of AHFS.

EXPERIMENTAL

In this study, zeolites Y purchased from Union Carbide (United States) and ZAO Nizhegorodskie sorbenty (Russia) were used; the zeolites had a crystal size of 1100 and 700 nm, respectively. Zeolites with a smaller crystal size were synthesized as described below.

Zeolite Y with a crystal size of 450 nm was synthesized by hydrothermal crystallization at a temperature of 70°C for 18 h from the reaction mixture having composition $4.6Na_2O : 1.0Al_2O_3 : 10SiO_2 : 180H_2O$ and containing 5 wt % of the seed. The precursors were a freshly precipitated silica hydrogel, sodium aluminate, sodium hydroxide, and distilled water. Zeolite Y with a crystal size of 300 nm was synthesized as described in [15, 16]. Zeolite Y with a crystal size of 50 nm was synthesized from the reaction mixture with composition $5.5(TMA)_2O : 2.3Al_2O_3 : 10SiO_2 : 570H_2O$ in two stages: at 40°C for 24 h and at 100°C for 48 h. The precursors were aluminum isopropoxide, an aqueous solution of tetramethylammonium hydroxide with a concentration of 25 wt %, and silica sol LUDOX HS-30 (30 wt %).

After zeolite crystallization, the treatments were as follows: the isolation and washing of nanocrystals to a pH of 9 by centrifugation and drying at 80°C for 6 h. All the samples, the commercial zeolites are among them, were subjected to three 3-h runs of ion exchange in an NH_4NO_3 solution at 80°C; after that, they were washed and dried at 80°C for 6 h.

The set of the synthesized samples was designated as FAU-N, where N is the average crystal size (in nm).

Dealumination with SHT was implemented in two stages. At the first stage, SHT was run at 550°C for 2 h; at the second stage, at 650°C for 2 h [17, 18]. Between the first and second treatments, the samples were subjected to ion exchange in an NH_4NO_3 solution at 80°C, with a duration of one run of 3 h, and subsequent washing and drying at 80°C. After the second SHT, the sample was washed in a nitric acid solution at 80°C to remove aluminum released from the tetrahedral positions of the framework.

The isomorphous substitution of Si for Al was implemented in an AHFS solution. The zeolite was suspended in a 3.4 M aqueous solution of ammonium acetate at 75°C. After that, AHFS was added dropwise to the suspension for 1 h; the resulting mixture was held at 75°C for 20 h. After the treatment, the zeolite was isolated from the suspension, washed by centrifugation, and dried at 80°C for 6 h.

The chemical composition of the samples was determined by X-ray fluorescence analysis (XRF) on a Thermo Scientific ARL Perform'X instrument with a 3.5-kW rhodium tube. Before analysis, 0.15- to 0.20-g portions of the samples were compressed into pellets with boric acid.

The X-ray diffraction (XRD) analysis of the samples was conducted on a Bruker D2PHASER instrument using CuK_α radiation. The diffraction patterns were recorded in a 2θ angular range of 5°–50° in increments of 0.05°. The Si/Al molar ratio was determined by the following formula [19]:

$$\mathrm{Si/Al} = \frac{1.7927}{\mathrm{UCS} - 24.238} - 1,$$

where UCS is the unit cell size of the zeolite.

The pore structure characteristics of the samples were determined by low-temperature nitrogen adsorption–desorption. Adsorption isotherms were recorded in accordance with the standard procedure on a Micromeritics ASAP 2010 porosimeter. The pore structure characteristics were calculated using the ASAP V2.00 dedicated software.

Electron microscopy images of the samples were recorded on a Hitachi TM3030 scanning electron microscope. Before recording, a layer of gold was deposited on the surface of the samples by vacuum deposition. High-resolution transmission electron microscope (TEM) micrographs were recorded on a JEOL JEM 2010 instrument at an accelerating voltage of 200 kV.

Magic-angle spinning nuclear magnetic resonance (MAS NMR) spectra were recorded on a Bruker Avance II 400 spectrometer at a magnetic field of 9.4 T. ^{1}H, ^{27}Al, and ^{29}Si NMR spectra were recorded. The spectra were processed and analyzed using Topspin 2.1 software. The calculation of Si/Al ratios according to the ^{29}Si spectra was conducted using the formula from [20]:

$$\mathrm{Si/Al} = \frac{\sum_{n=0}^{4} I_{\mathrm{Si}(n\mathrm{Al})}}{\sum_{n=0}^{4} 0.25 n I_{\mathrm{Si}(n\mathrm{Al})}},$$

where $I_{\mathrm{Si}(n\mathrm{Al})}$ is the intensity of the signal of silicon surrounded by n Al atoms, i.e. $\mathrm{Si(OSi)}_{4-n}\mathrm{(OAl)}_n$.

RESULTS AND DISCUSSION

The physicochemical characteristics of the synthesized zeolite Y samples are shown in Table 1. Accord-

Table 1. Physicochemical properties of the samples

Sample	Dealumination method	Si/Al			Pore volume		XRD		Average crystal size, nm
		XRF	XRD	^{29}Si NMR	V_{tot}, cm^3/g[a]	V_{mic}, cm^3/g[b]	Unit cell size, Å	Phase	
FAU-1100	–	2.8	3.1	2.7	0.330	0.307	24.68	FAU (Y)	1100
	SHT	9.6	80.5	–	0.331	0.159	24.26	FAU (Y)	
	AHFS	4.7	5.0	4.5*	0.274	0.249	24.54	FAU (Y)	
FAU-700	–	2.8	2.6	2.7	0.316	0.273	24.73	FAU (Y)	700
	SHT	7.6	41.7	–	0.374	0.196	24.28	FAU (Y)	
	AHFS	4.2	8.3	4.2*	0.265	0.220	24.43	FAU (Y)	
FAU-450	–	2.1	2.6	2.1	0.331	0.324	24.74	FAU (Y)	450
	SHT	amorphization							
	AHFS	4.3	5.6	3.7*	0.302	0.282	24.51	FAU (Y)	
FAU-300	–	1.8	2.0	1.6	0.335	0.245	24.83	FAU (Y)	300
	SHT	amorphization							
	AHFS	3.1	4.5	3.3*	0.238	0.154	24.56	FAU (Y)	
FAU-50	–	1.7	1.9	1.6	0.191	0.130	24.85	FAU (Y)	50
	SHT	amorphization							
	AHFS	3.3	3.8	3.1*	0.174	0.300	24.61	FAU (Y)	

* NMR data give underestimated Si/Al values for the dealuminated samples because of a large number of defects, such as $Si(OAl)_3OH$ and $Si(OAl)_2(OH)_2$, which are formed during dealumination.
[a] Total pore volume.
[b] Micropore volume.

ing to XRD and low-temperature nitrogen adsorption, all the as-synthesized samples are highly crystalline zeolites with the FAU(Y) structure. The Si/Al ratio decreases in proportion to a decrease in the crystal size. The Si/Al values determined by the XRF and ^{29}Si solid-state NMR methods (Table 1) are in good agreement with each other. It is significant that, regardless of the crystal size, all the freshly synthesized samples contain no extraframework 6-coordinated aluminum corresponding to a signal at ca. 0 ppm (Fig. 1a). Thus, all the aluminum is located in the zeolite Y framework, which corresponds to a distinct narrow signal at 61 ppm [21].

The dealumination of samples with large crystals by the SHT method leads to a significant increase in the Si/Al ratio (Table 1) and a decrease in the degree of crystallinity, as shown in Fig. 2 (curve *2*) using the example of the FAU-700 sample. The samples with a crystal size of 450 nm or less undergo complete amorphization during the SHT; this finding is consistent with the data reported in [22]. This effect is apparently attributed to the fact that, at a lower initial Si/Al ratio (1.7–2.1 in the FAU-50–FAU-450 samples), the crystal structure is not sufficiently resistant to the removal of a large portion of aluminum; as a consequence, it undergoes amorphization. In the FAU-1100 and FAU-700 samples, degradation does not occur; however, the micropore volume significantly decreases (Table 1); this decrease is consistent with the decrease in the degree of crystallinity. It is of interest that the isotherm of the FAU-700 sample obtained after SHT dealumination has a shape characteristic of mesoporous materials (Fig. 3, curve *2*). In this case, hysteresis is observed; this fact indicates the formation of bottle-shaped pores. This effect can be attributed to both the fact that dealumination occurs not only on the surface but also in the bulk of the crystals and the fact that the alumina phase formed during SHT partially blocks the micropores.

The ^{27}Al MAS NMR spectra (Fig. 1b) show that the SHT leads to the partial exit of aluminum atoms from the tetrahedral positions of the framework into the extraframework state, which is accompanied by the appearance of signals in the spectra at 30 and 0 ppm, which correspond to 5- and 6-coordinated aluminum. Therefore, the degree of dealumination determined from the elemental composition is significantly lower than the real degree of dealumination. Since a change in the unit cell size is sensitive only to a change in the Si/Al ratio in the zeolite structure, the values determined from XRD data give a more accurate estimate than the gross composition determined by chemical analysis. Thus, according to XRD, the Si/Al ratio provided by dealumination for the FAU-1100 and FAU-700 samples can be estimated as 80.5 and 41.7, respectively.

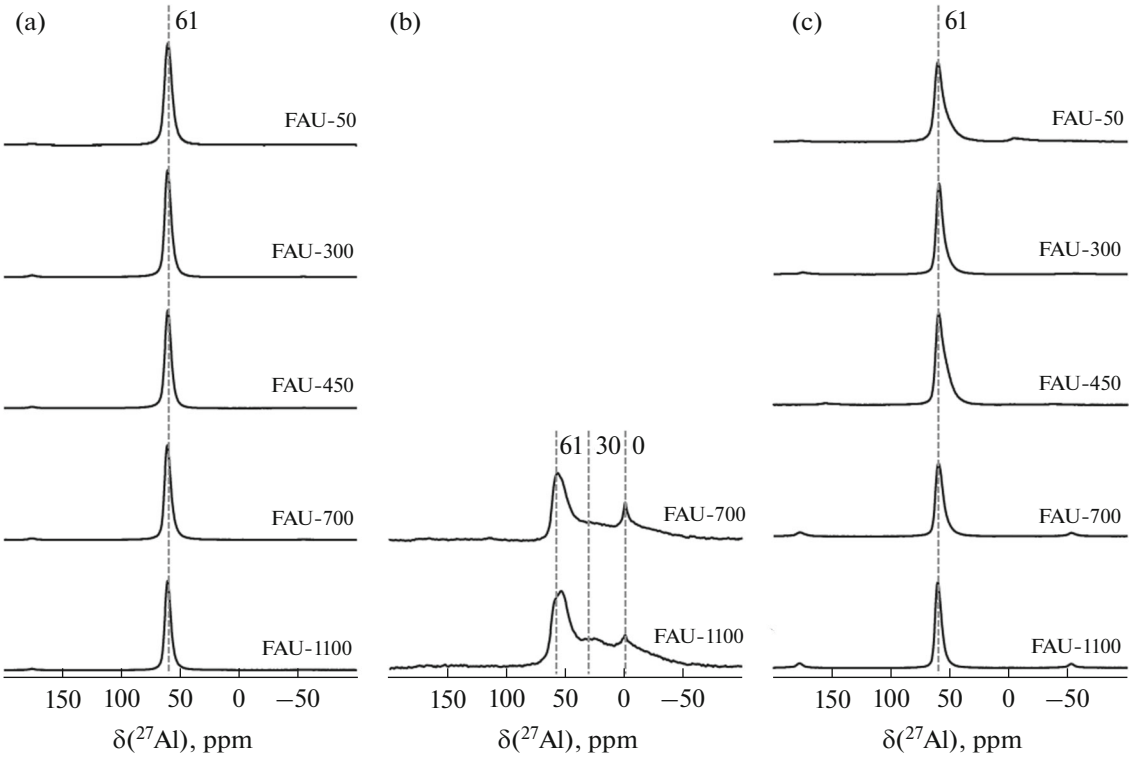

Fig. 1. ^{27}Al solid-state NMR spectra for (a) as-synthesized samples with different crystal sizes and the samples dealuminated by the (b) SHT and (c) AHFS methods.

According to XRF, dealumination by AHFS treatment is gentler than dealumination with SHT; the Si/Al molar ratio in the samples varies from 1.7–2.8 to 3.3–4.7 (Table 1). At the same time, the degree of crystallinity of the synthesized samples remains almost unchanged (Fig. 2, curve *3*); almost all the aluminum remains in the zeolite framework, as evidenced by the preservation of signal intensities in the ^{27}Al NMR spectra (Fig. 1c). However, as in the case of SHT, treatment with AHFS leads to a certain decrease in the surface area and volume of micropores (Table 1). At the same time, the micropore volume in the zeolite samples after treating with AHFS is larger than that after SHT, as shown by the data obtained for FAU-1100 and FAU-700 (Table 1). This finding is attributed to the mechanism of action of AHFS, where the healing of crystal defects occurs via the isomorphous substitution of framework aluminum by silicon [11].

According to TEM (Fig. 4a), the AHFS treatment leads to the formation of a SiO_2 film on the crystal surface; the film is clearly visible in the images obtained. For the smaller crystals, this film contributes to the coalescence of crystals (Fig. 4b); therefore, the decrease in the surface area is more pronounced. According to the shape of the nitrogen adsorption isotherm (Fig. 3, curve *3*), during treatment with AHFS, unlike SHT, no mesopores are formed. The shift of the isotherm to the region of smaller sorbed volumes and the occurrence of hysteresis can indicate both a partial blocking of the pores and a decrease in the pore diameter. This feature makes this method less promising for synthesizing highly efficient catalysts.

The data in Table 1 show that the AHFS treatment can be used to provide a partial dealumination of nanocrystalline zeolite Y with a crystal size of 50 nm. During the modification, the Si/Al ratio varies from 1.7 to 3.3, which corresponds to a degree of dealumination of 36.7%.

Thus, comparison of the dealumination of zeolites Y with different crystal sizes by the SHT and AHFS methods has shown the following. Under the selected conditions, SHT provides a deep dealumination of zeolites Y with a crystal size of more than 700 nm up to a Si/Al ratio in the framework of 40–80. The use of this method for zeolites Y with a crystal size of less than 700 nm is restricted, because it leads to the complete amorphization of the zeolites. The treatment with AHFS, in turn, makes it possible to gently dealuminate zeolites Y to a Si/Al ratio in the framework of 3.8–5.0, while preserving the high crystallinity of the samples and the tetrahedral state of aluminum in the framework. It has been shown for the first time that nanocrystalline zeolite Y with a crystal size of 50 nm can be subjected to this modification. A disadvantage of the AHFS treatment is formation of the SiO_2 film

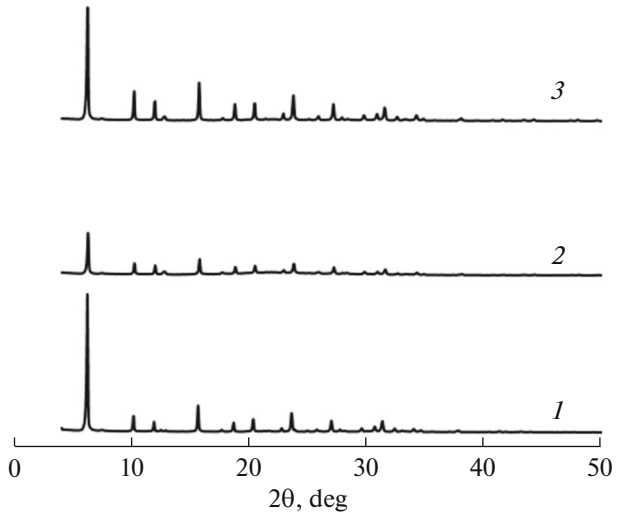

Fig. 2. Diffraction patterns of the FAU-700 sample (*1*) in the as-synthesized form and after dealumination by the (*2*) SHT and (*3*) AHFS methods.

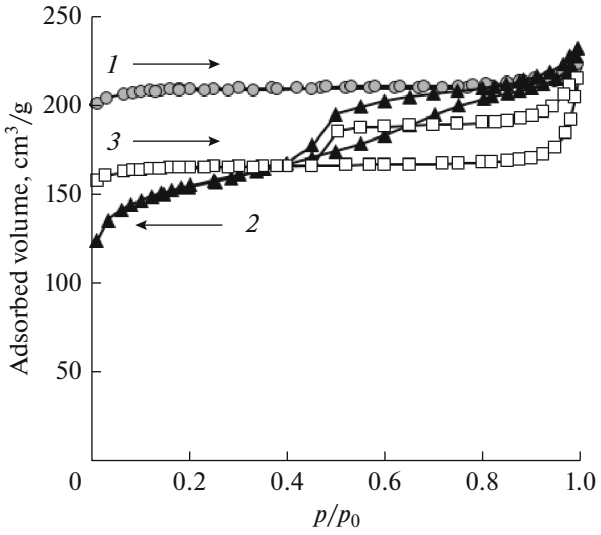

Fig. 3. Low-temperature nitrogen adsorption isotherms of the FAU-700 sample (*1*) in the as-synthesized form and after dealumination by the (*2*) SHT and (*3*) AHFS methods.

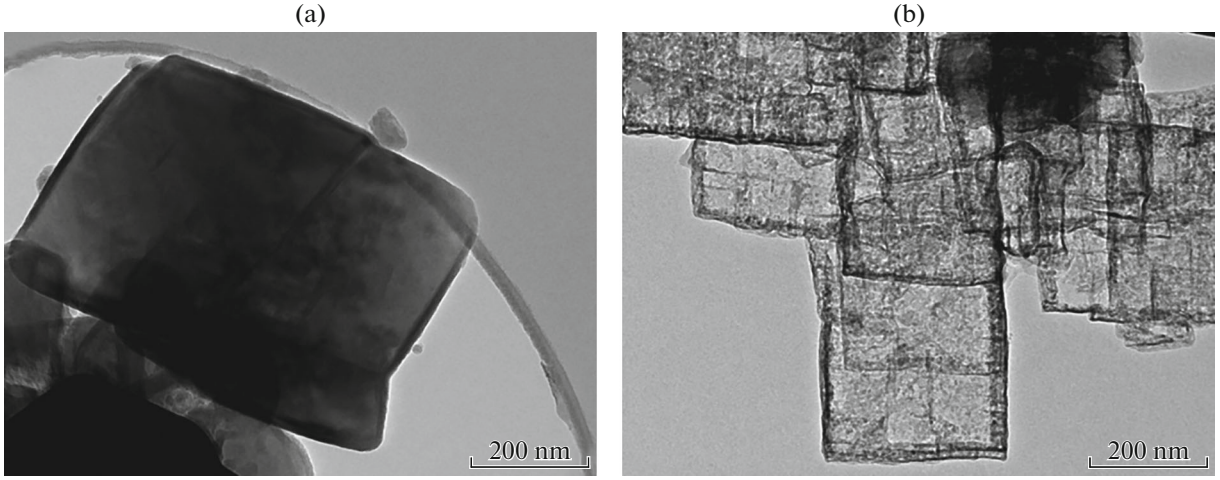

Fig. 4. Transmission electron microscopy micrographs for the (a) FAU-450 and (b) FAU-300 samples dealuminated by the treatment with AHFS.

on the crystal surface; this feature significantly restricts the use of this method for synthesizing catalysts based on dealuminated zeolites Y.

ACKNOWLEDGMENTS

This work was supported by the Russian Science Foundation (project no. 14-23-00094).

REFERENCES

1. *Zeolites and Catalysis: Synthesis, Reactions and Applications*, Ed. by J. Cejka, A. Corma, and S. Zones (Wiley, Weinheim, 2010).
2. J. Scherzer, Catal. Rev.–Sci. Eng. **31** (3), 215 (1989).
3. D. W. Breck, *Zeolite Molecular Sieves: Structure, Chemistry, and Use* (Wiley, New York, 1984).
4. R. M. Barrer, *Hydrothermal Chemistry of Zeolites* (Academic Press, London, 1982).
5. D. E. W. Vaughan, G. C. Edwards, and M. G. Barrett, U.S. Patent No. 4 178 352 (1979).
6. C. V. McDaniel and H. C. Duecker, U.S. Patent No. 3 574 538 (1971).
7. J. Scherzer, J. Catal. **54** (2), 285 (1978).
8. H. Najar, M. Zina, and A. Ghorbel, React. Kinet. Mech. Catal. **100** (2), 385 (2010).
9. C. S. Triantafillidis, A. G. Vlessidis, and N. P. Evmiridis, Ind. Eng. Chem. Res. **39** (2), 307 (2000).

10. Q. L. Wang, G. Giannetto, M. Torrealba, G. Perot, C. Kappenstein, and M. Guisnet, J. Catal. **130** (2), 459 (1991).
11. G. W. Skeels and D. W. Breck, in *Proceedings of the 6th International Zeolite Conference, Reno, United States, 1984*, p. 87.
12. B. Chauvin, M. Boulet, P. Massiani, F. Fajula, F. Figueras, and T. Des Courieres, J. Catal. **126** (2), 532 (1990).
13. S. C. Larsen, J. Phys. Chem. **111** (50), 18 464 (2007).
14. B. A. Holmberg, H. Wang, and Y. Yan, Microporous Mesoporous Mater. **74** (1–3), 189 (2004).
15. Y. Huang, K. Wang, D. Dong, D. Li, M. R. Hill, A. J. Hill, and H. Wang, Microporous Mesoporous Mater. **127** (3), 167 (2010).
16. E. E. Knyazeva, A. V. Yakimov, O. V. Shutkina, S. V. Konnov, A. V. Panov, A. V. Kleimenov, D. O. Kondrashev, V. A. Golovachev, and I. I. Ivanova, Pet. Chem. **56** (12), 1168 (2016).
17. B. Chauvin, M. Boulet, P. Massiani, F. Fatula, F. Figueras, and T. D. Courieres, J. Catal. **126** (2), 532 (1990).
18. D. W. Breck and G. W. Skeels, U.S. Patent No. 4 053 023 (1985).
19. J. R. Sohn, S. J. DeCanio, J. H. Lunsford, and D. J. O'Donnell, Zeolites **6** (3), 225 (1986).
20. H. Van Bekkum, E. M. Flanigen, P. A. Jacobs, and J. C. Jansen, *Introduction to Zeolite Science and Practice* (Elsevier, Amsterdam, 2001).
21. J. Rocha and J. Klinowski, J. Chem. Soc., Chem. Commun., No. 16, 1121 (1991).
22. R. A. Rakoczy and Y. Traa, Microporous Mesoporous Mater. **60** (1–3), 69 (2003).

Translated by M. Timoshinina